Dynamic Nuclear Spin Polarization in the Resonant Laser Excitation of an InGaAs Quantum Dot

A. Högele[1], M. Kroner[2], C. Latta[2,3], M. Claassen[4], I. Carusotto[5], C. Bulutay[2,6], and A. Imamoglu[2]

[1]*Fakultät für Physik and CeNS, Ludwig-Maximilians-Universität München, D-80539 München, Germany*
[2]*Institute of Quantum Electronics, ETH Zürich, CH-8093, Zürich, Switzerland*
[3]*Physics Department, Harvard University, 17 Oxford St., Cambridge, Massachusetts 02138, USA*
[4]*Department of Applied Physics, Stanford University, Stanford, California 94305, USA*
[5]*INO-CNR BEC Center and Dipartimento di Fisica, Università di Trento, I-38123 Povo, Italy and*
[6]*Department of Physics, Bilkent University, Ankara, 06800, Turkey*

Supplementary online material

Description of the experiment

A voltage applied to the Schottky top gate was used to tune the QD into stable charge configurations with the ground state being singly positively charged, neutral or singly negatively charged [1, 2]. Single electrons were injected into the QD from the Fermi reservoir, whereas in absence of a hole reservoir in the device, single hole injection was ensured by the presence of a weak nonresonant laser. The sample was cooled in a bath cryostat to liquid helium temperature (4.2 K) and finite magnetic fields were applied in Faraday or Voigt configuration, parallel or perpendicular to the sample growth axis z, respectively.

Resonant absorption of the neutral exciton X^0 as well as positive and negative trions, X^+ and X^-, was probed with a tunable narrow-band laser in differential transmission spectroscopy [3]. Absorption spectra were recorded by setting the gate voltage or the laser energy to a specific detuning $\Delta = \omega_X - \omega_L$, waiting for a time t_c and monitoring the transmission signal with a lock-in amplifier. After each measurement, the voltage/laser energy was changed by a discrete detuning step Δ_n.

In finite magnetic fields, QDs in both samples A and B showed pronounced dragging. QDs in sample A, for example, exhibited dragging of both X^0 and X^- in the range of tens of μeV in contrast to QDs of sample B with sub 10 μeV scale for both trions. The thickness of the tunnel barrier strongly affects electron spin exchange with the Fermi reservoir via cotunneling [4] and thus the efficiency of DNSP [5]. In particular, in sample B the dragging widths of X^- are reduced due to strong spin pumping at magnetic fields exceeding ≈ 0.3 T [6]. In Voigt geometry the spin pumping leads to a significant reduction in the transmission contrast and consequently in the dragging efficiency even at the edge of the charging plateau. However, the X^0 of the same QD from sample B exhibited a ≈ 20 μeV dragging width, consistent with the findings from sample A. For X^+ the reduced DNSP range is consistent with the presence of a nonresonant laser which not only injects holes into the ground state of X^+ but also non-geminate electron spins opening up an additional nuclear spin decay channel. The nuclear spin polarization is therefore reduced for (photo-generated) single-hole-charged initial states.

Non-collinear hyperfine interaction

The effective noncollinear hyperfine interaction Hamiltonian stems from the fact that the quadrupolar interaction Hamiltonian for a nuclear spin with strain axis tilted by an angle θ from the z-axis (in the $x - z$ plane)

$$\hat{H}_{quad} = B_Q[\hat{I}_z^2 \cos^2\theta + (\hat{I}_z\hat{I}_x + \hat{I}_x\hat{I}_z)\sin\theta\cos\theta + \hat{I}_x^2 \sin^2\theta] \tag{1}$$

does not commute with the dominant $\hat{H}_{fc,z} = \sum_i 2A_i\hat{I}_z^i\hat{S}_z$ term of the Fermi-contact hyperfine interaction $\hat{H}_{fc}$. To obtain an analytic expression for A_i^{nc}, we assume $\theta \ll 1$ and use a Schrieffer-Wolff (SW) transformation to obtain $\hat{H}_{hyp} = \hat{H}_{fc} + \hat{H}_{hyp-quad}$ where

$$\hat{H}_{hyp-quad} = \sum_i A_i^{nc}\hat{S}_z[\hat{I}_x^i\hat{I}_z^i + \hat{I}_z^i\hat{I}_x^i] , \tag{2}$$

with $A_i^{nc} = A_iB_Q^i\sin(2\theta_i)/\omega_Z^n$. In $\hat{H}_{hyp-quad}$ we have only kept the terms that describe processes which leave the electron spin-state unchanged, since contributions that flip the electron spin will be negligible at high external fields. Finally, we note that even for large B_z, the dominant role of flip-flop terms of Fermi-contact hyperfine interaction is to induce indirect interaction between the QD nuclei [7]: the primary effect of this interaction, in the presence of fast optical dephasing of the electonic spin resonance, is to ensure that the nuclear spin population assumes a thermal distribution on timescales fast compared to the polarization timescale determined by A_i^{nc}. In this limit, the dynamics due to $\hat{H}_{hyp-quad}$ will be indistinguishable from that described by $\hat{H}_{nc}$.

Averaging over the distribution for nuclei that lie within the Gaussian QD electron wavefunction, we obtain for cations (In and Ga with 9/2 and 3/2 nuclear spins, respectively, and $A^{In} = 112$ μeV, $A^{Ga} = 84$ μeV [8]) $A_i^{nc} \simeq 0.0124 \cdot A^{In,Ga}$ and for anions (As with 3/2 nuclear spin and $A^{As} = 92$ μeV [8]) $A_i^{nc} \simeq 0.0848 \cdot A_i^{As}$. For a fully polarized $In_{0.7}Ga_{0.3}As$ system we determine the value for the maximum Overhauser splitting due to the noncollinear hyperfine coupling as $A^{nc} = 0.0124 \cdot 0.5 \cdot (0.7 \cdot \frac{9}{2}A^{In} + 0.3 \cdot \frac{3}{2}A^{Ga}) + 0.0848 \cdot 0.5 \cdot \frac{3}{2}A^{As} \simeq 8.27$ μeV and obtain an average value of $A_i^{nc} \simeq 2.6 \cdot 10^{-4}$ μeV with $N = 3.2 \cdot 10^4$.
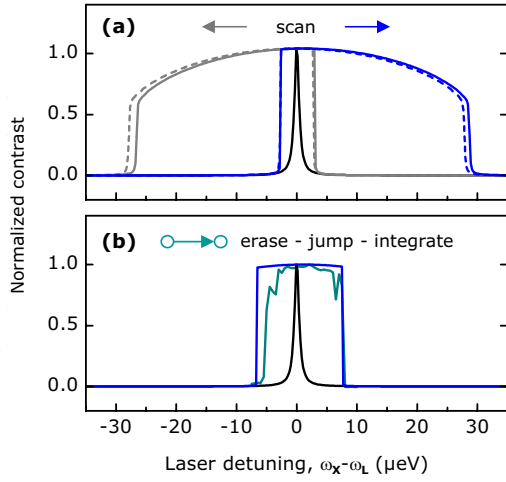
FIG. 1: (a) Simulations of dynamic dragging as in Fig. 1 of the manuscript yet without spectral jitter: the solid and dashed lines represent steady state solutions for scans ($t_c = 0.2$ s and $\Delta_n = 0.23$ μeV) with and without spin-flip Raman scattering processes according to Eqn.s 5 and 3, respectively. The slight asymmetry to positive laser detunings is a result of directional dynamic nuclear spin polarization stemming from spin-flip Raman processes. (b) Comparison between experimental spectra (dark cyan) and results of the simulation (blue) for sequential data acquisition ($t_c = 60$ s and $\Delta_n = 0.46$ μeV): each data point of the spectra was obtained by (i) erasing the nuclear spin polarization in a voltage region with strong cotunneling, (ii) subsequently establishing a finite laser detuning, and (iii) integrating for the time t_c at this specific detuning. The Lorentzian spectra in (a) and (b) are calculated with $\Gamma_0 = 0.73$ μeV and shown in black for reference.

Modelling of the experimental data

To obtain a quantitative prediction, we consider the rate equation

$$\frac{dI_z}{dt} = W_+(I_z)(\frac{N}{2} + I_z) - W_-(I_z)(\frac{N}{2} - I_z) - \Gamma_d I_z, \quad (3)$$

where

$$\Gamma_d = \Gamma_0 \left(\frac{A_i^{nc}}{2\omega_Z^n}\right)^2 \frac{\Omega^2/4}{\delta^2 + \Gamma_0^2/4 + \Omega^2/2} \quad (4)$$

is the rate at which nuclear-spin-flip assisted spontaneous emission, leading to pure nuclear spin diffusion, takes place. Here, as well as in the following equation, $\delta = \Delta - A_i I_z$. The rate equation yields symmetric dragging [dashed spectra in Fig. 1(a)] and antidragging to either side of the resonance for the blue and red Zeeman branches, respectively, qualitatively similar to the results of Yang and Sham [9].

Taking into account uni-directional spin-flip Raman scattering processes that arise from the Fermi-contact hyperfine interaction, we arrive at a refined rate equation model:

$$\begin{aligned}\frac{dI_z}{dt} &= W_+(I_z)(\frac{N}{2} + I_z) - W_-(I_z)(\frac{N}{2} - I_z) - \Gamma_d I_z \\ &\quad - \Gamma_{sf}(\frac{N}{2} + I_z)\end{aligned} \quad (5)$$
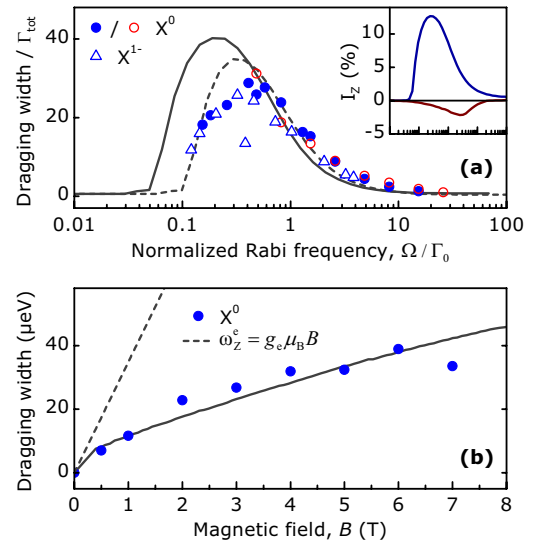
FIG. 2: (a) Laser power dependence of the maximum dragging width in forward scans at $B = 4.5$ T for the neutral exciton X^0 (blue Zeeman branch: closed circles; red Zeeman branch: open circles) and the negative trion X^- (open triangles) in sample A. The dragging width is normalized to the power-broadened total linewidth Γ_{tot}, the laser power is expressed as Ω/Γ_0 (with experimentally determined radiative decay rates $\Gamma_0 = 0.8$ ns^{-1} for X^0 and 1.1 ns^{-1} for X^-). The results of the model are shown by the solid line for Ω/Γ_0 and dashed line for $\Omega/(2\Gamma_0)$. The inset shows on the same abscissa scale in red and blue the corresponding degree of nuclear spin polarization accumulated in a forward scan at initially negative and positive laser detunings, respectively. Small but finite degree of nuclear spin polarization at high laser powers stems from directional spin-flip Raman scattering processes. (b) Maximum dragging width of X^0 (circles) as a function of magnetic field for $\Omega \simeq 0.5\Gamma_0$. The sub-linear monotonic increase of the maximally achieved dragging width is reproduced by the simulations (solid line). The linearly increasing electron Zeeman energy ω_Z^e is also shown (dashed line).

with

$$\Gamma_{sf} = \Gamma_0 \left(\frac{A_i}{4\omega_Z^e}\right)^2 \frac{\Omega^2/4}{\delta^2 + \Gamma_0^2/4 + \Omega^2/2}. \quad (6)$$

Spin-flip Raman scattering processes at rate Γ_{sf} give rise to the asymmetry in the spectra for forward and reverse scan directions (compare solid and dashed spectra in Fig. 1(a)), in agreement with experimental findings. The argument for the asymmetry holds when the nuclear spin polarization is erased before a sudden jump to a finite detuning and subsequent build-up of DNSP [5]: locking of the resonance extends further for positive laser detunings [Fig. 1(b)]. Moreover, spin-flip Raman scattering processes ensure small but finite nuclear spin polarization at high laser powers, as shown in the inset of Fig. 2(a).

The normalized absorption spectra depicted in Fig. 1(a) are calculated from steady state solutions of Eqn.s 3 and 5 with the following parameters: $\hbar\Gamma_0 = 0.7$ μeV from the radiative decay rate $1/\Gamma_0 = 1.2$ ns determined from saturation [10], $\Omega = 0.5\,\Gamma_0$, $B = 4.5$ T, step size $\Delta_n = 0.23$ μeV

and dwell time $t_c = 0.2$ s, as used in the experiments, and $\omega_Z^e/\omega_Z^n = 1000$, $N = 3.2 \cdot 10^4$, $A_i = 120$ μeV$/N$, $A_i^{nc} = 0.45 \cdot 10^{-4}$ μeV. Intrinsic decay of the nuclear spin polarization is negligible for the ground state of X^0 [7, 11]. Here, we omitted the unbalanced telegraph noise in the resonance condition used to calculate the spectra in Fig. 1 of the manuscript. This jitter in the resonance condition with an amplitude of 0.5 μeV (smaller than the linewidth) and timescales longer than t_c was included in simulations in order to account for the asymmetry observed experimentally for the two scan directions. It is consistent with the spectral fluctuations in resonant QD spectroscopy [10]. Based on experimental observations for the QDs in sample A, it is reasonable to assume these fluctuations to be unbalanced with a small weight on the higher energy side of the resonance. However, comparing the observed traces for different QDs in different samples reveals that the spectral jitter can actually appear on either side of the resonance.

The dependence of the dragging width on the magnitude of the laser power and the external magnetic field provides further confirmation of the model. Fig. 2 shows how the dragging width evolves as a function of laser power and magnetic field. The effect of dragging is inhibited at low incident powers, increases until reaching a maximum below the saturation at $\Omega \simeq \Gamma_0$, and vanishes in the limit of high excitation powers [Fig. 2(a)]. This is consistent with the prediction of Eq.s 3 and 5: the maximum dragging width is expected at $\Omega < \Gamma_0$ for non-vanishing Γ_d and Γ_{sf}. Both X^0 and X$^-$ reveal the same dependence when the dragging width on the ordinate is normalized to the total linewidth $\Gamma_{tot} = \sqrt{\Gamma_0^2 + \Omega^2/2}$ and the abscissa is expressed is units of Ω/Γ_0. The results of the model reproduce our experimental findings [solid line in Fig. 2(a)] predicting ~ 10 % of nuclear spin polarization at maximum [inset of Fig. 2(a)]. The model overestimates the dragging width at powers below saturation but gives perfect agreement above saturation for $\tilde{\Omega} = \Omega/2$. We speculate that the scaling factor of 2 stems from the line broadening $\Gamma \simeq 2\,\Gamma_0$ that we typically find in our samples as a result of spectral fluctuations [10]. The monotonic sublinear increase of the dragging width with magnetic field, as measured on X^0 close to saturation, is clearly reproduced by our model [solid line in Fig. 2(b)] and provides further confirmation for the quantitative nature of our analysis.

———————

[1] R. J. Warburton *et al.*, Nature (London) **405**, 926 (2000)
[2] S. Seidl *et al.*, Phys. Rev. B **72**, 195339 (2005).
[3] B. Alen *et al.*, Appl. Phys. Lett. **83**, 2235 (2003).
[4] J. M. Smith *et al.*, Phys. Rev. Lett. **94**, 197402 (2005).
[5] C. Latta *et al.*, Nature Phys. **5**, 758 (2009).
[6] M. Atatüre *et al.*, Science **312**, 551-553 (2006).
[7] C. Latta, A. Srivastava, and A. Imamoglu, Phys. Rev. Lett. **107**, 167401 (2011).
[8] P.-F. Braun *et al.*, Phys. Rev. B **74**, 245306 (2006).
[9] W. Yang and L. J. Sham, arXiv:1012.0060 (2010).
[10] A. Högele *et al.*, Phys. Rev. Lett. **93**, 217401 (2004).
[11] P. Maletinsky, M. Kroner, and A. Imamoglu, Nature Phys. **5**, 407 (2009).